

See discussions, stats, and author profiles for this publication at: <https://www.researchgate.net/publication/228485133>

Correlation and Prediction of Phase Behavior of Organic Compounds in Ionic Liquids Using the Nonrandom Two-Liquid Segment Activity Coefficient Model

ARTICLE *in* INDUSTRIAL & ENGINEERING CHEMISTRY RESEARCH · SEPTEMBER 2008

Impact Factor: 2.59 · DOI: 10.1021/ie800048d

CITATIONS

22

READS

41

4 AUTHORS, INCLUDING:



Chau-Chyun Chen

Texas Tech University

92 PUBLICATIONS 3,367 CITATIONS

SEE PROFILE



Luke Simoni

The Chemours Company

18 PUBLICATIONS 354 CITATIONS

SEE PROFILE

Article

Correlation and Prediction of Phase Behavior of Organic Compounds in Ionic Liquids Using the Nonrandom Two-Liquid Segment Activity Coefficient Model

Chau-Chyun Chen, Luke D. Simoni, Joan F. Brennecke, and Mark A. Stadtherr

Ind. Eng. Chem. Res., **2008**, 47 (18), 7081-7093 • DOI: 10.1021/ie800048d • Publication Date (Web): 14 August 2008

Downloaded from <http://pubs.acs.org> on April 2, 2009

More About This Article

Additional resources and features associated with this article are available within the HTML version:

- Supporting Information
- Access to high resolution figures
- Links to articles and content related to this article
- Copyright permission to reproduce figures and/or text from this article

[View the Full Text HTML](#)



ACS Publications
High quality. High impact.

Correlation and Prediction of Phase Behavior of Organic Compounds in Ionic Liquids Using the Nonrandom Two-Liquid Segment Activity Coefficient Model

Chau-Chyun Chen,^{*,†} Luke D. Simoni,[‡] Joan F. Brennecke,[‡] and Mark A. Stadtherr^{*}

Aspen Technology, Inc., Burlington, Massachusetts 01803, and Department of Chemical and Biomolecular Engineering, University of Notre Dame, Notre Dame, Indiana 46556

Room-temperature ionic liquids have shown great potential as media for reactions and separations. Information on how organic compounds interact with these ionic liquids is crucial in assessing their usefulness. Here, the nonrandom two-liquid segment activity coefficient (NRTL-SAC) model is used first to correlate values of infinite-dilution activity coefficients for organic compounds in ionic liquids and then to predict the phase behavior of various mixtures involving these ionic liquids. NRTL-SAC provides a robust, qualitative predictive model based on four molecular descriptors that are designed to capture molecular surface interaction characteristics: hydrophobicity, hydrophilicity, polarity, and solvation strength.

Introduction

Ionic liquids (ILs) are organic electrolytes that remain as liquid at temperatures less than 100 °C, e.g., at room temperature. Ionic liquids have shown great potential as media for reactions and separations. Information on how solvents interact with these ionic liquids and the resulting phase behavior for solvent–ionic liquid mixtures is crucial in assessing their usefulness. Infinite-dilution activity coefficients, γ^∞ , of solvents in ionic liquids provide useful information about such solvent–ionic liquid intermolecular interactions, and the screening of solvents for potential application in solvent-enhanced separation processes of organic liquid mixtures can be achieved through the examination of the infinite-dilution activity coefficients of solvents.¹ Diedenhofen et al.² recently applied COSMO-RS to give a priori predictions of infinite-dilution activity coefficients for 38 compounds in three ionic liquids, i.e., 1-methyl-3-ethylimidazolium bis((trifluoromethyl)sulfonyl)imide, 1,2-dimethyl-3-ethylimidazolium bis((trifluoromethyl)sulfonyl)imide, and 4-methyl-*N*-butylpyridinium tetrafluoroborate. They showed COSMO-RS predicts the infinite-dilution activity coefficients in various ionic liquids with the same accuracy that is observed for those in normal organic solvents. Eike et al.³ later applied the quantitative structure–property relationship (QSPR) method to correlate and predict values of infinite-dilution activity coefficients for the same solvent–ionic liquid systems using four descriptors. They have shown the QSPR method to be predictive and a powerful tool for extending experimental activity coefficient data. More recently, Banerjee and Khanna⁴ reported experimental infinite-dilution activity coefficient measurements and compared the COSMO-RS predictions favorably against the experimental data for three trihexyltetradecylphosphonium cation-based ionic liquids. Also, Freire et al.⁵ observed a reasonable qualitative agreement between COSMO-RS predictions and experimental binary VLE and LLE measurements in some IL–alcohol systems.

The nonrandom two-liquid segment activity coefficient model (NRTL-SAC) is a simple molecular thermodynamic framework that characterizes molecular interaction characteristics in terms of four dimensionless molecular descriptors: hydrophobicity,

hydrophilicity, polarity, and solvation strength.⁶ While the model was first developed for nonelectrolytes, it was later extended for electrolytes.⁷ Using NRTL-SAC, one would first identify the molecule-specific parameters, i.e., molecular descriptors, for the compound of interest by using phase equilibrium data such as compound solubilities in a few reference solvents or infinite-dilution activity coefficients of solvents in the compound or vice versa. The model can then be used to predict qualitatively the phase behavior of mixtures containing the compound as long as the molecular descriptors for other species in the mixture are also available. The model has been shown recently^{8–11} to deliver robust qualitative predictions for drug molecule solubilities in solvents and solvent mixtures within a factor of 2. This is an accuracy that is effective for solvent selection and active pharmaceutical ingredient process design in the pharmaceutical industry.¹¹

The goal of this work is to investigate the applicability of NRTL-SAC for ionic liquids. Although ionic liquids are made up of ionic species, they form molecular ion pairs and often exhibit phase behavior similar to that of molecular species. In this study, we treat ionic liquids as molecular species and we examine the ability of NRTL-SAC to correlate γ^∞ values for various organic solvents in ionic liquids. A more rigorous approach would be to model explicitly the chemical equilibrium between individual ions and ion pairs derived from ionic liquids and to apply the electrolyte NRTL-SAC model⁷ to all species in the solution. However, the chemical equilibrium constants between individual ions and ion pairs for ionic liquids are not readily available. The NRTL-SAC approach should be considered as a reasonable first approximation before more rigorous treatments are considered.

We focus on organic solvents with known NRTL-SAC parameters, and given the available γ^∞ data for the solvents in ILs, we identify NRTL-SAC parameters for ionic liquids. We then use these parameters to make phase behavior predictions for these solvent–IL mixtures, and we examine the quality of the predictions. In addition, the NRTL-SAC molecular parameters for the ILs are analyzed to decipher how IL molecular structure relates to molecular surface interaction characteristics in terms of hydrophobicity, hydrophilicity, polarity, and solvation strength.

In the following sections, we provide a brief summary of the NRTL-SAC model and explain the methodology through which correlation of minimal experimental γ^∞ data for organic solvents

* To whom correspondence should be addressed. E-mail: chauchyun.chen@aspentech.com.

[†] Aspen Technology, Inc.

[‡] University of Notre Dame.

Table 1. List of Organic Solvents and Their NRTL-SAC Molecular Descriptors

solvent	NRTL-SAC model parameters			
	X	Y−	Y+	Z
alkanes				
<i>n</i> -pentane	0.898	0.000	0.000	0.000
<i>n</i> -hexane	1.000	0.000	0.000	0.000
<i>n</i> -heptane	1.152	0.000	0.000	0.000
<i>n</i> -octane	1.253	0.000	0.000	0.000
cyclohexane	0.892	0.000	0.000	0.000
methylcyclohexane	1.053	0.000	0.246	0.000
alkylbenzenes				
benzene	0.615	0.000	0.281	0.000
toluene	0.604	0.000	0.304	0.000
xylene	0.758	0.021	0.316	0.000
ethylbenzene	0.715	0.000	0.343	0.000
polar organics				
acetone	0.131	0.109	0.513	0.000
2-butanone	0.261	0.095	0.463	0.000
2-pentanone	0.344	0.063	0.445	0.000
acetonitrile	0.018	0.131	0.883	0.000
1,4-dioxane	0.154	0.086	0.401	0.000
tetrahydrofuran	0.235	0.040	0.320	0.000
diisopropyl ether	0.584	0.071	0.093	0.000
methyl tert-butyl ether	0.483	0.105	0.142	0.000
ethyl acetate	0.339	0.058	0.441	0.000
<i>N</i> -methylpyrrolidone	0.252	0.790	0.281	0.000
<i>N,N</i> -dimethyl-formamide	0.180	0.752	0.254	0.000
alcohols				
methanol	0.090	0.139	0.000	0.594
ethanol	0.251	0.030	0.000	0.630
1-propanol	0.374	0.013	0.000	0.530
2-propanol	0.366	0.091	0.000	0.391
1-butanol	0.425	0.004	0.000	0.490
<i>sec</i> -butanol	0.343	0.069	0.000	0.393
<i>tert</i> -butanol	0.317	0.000	0.010	0.359
1-pentanol	0.458	0.024	0.000	0.491
<i>tert</i> -pentanol	0.388	0.482	0.000	0.203
cyclohexanol	0.616	0.064	0.000	0.556
chloromethanes				
dichloromethane	0.459	0.000	0.427	0.038
trichloromethane	0.393	0.000	0.167	0.000
tetrachloromethane	0.739	0.027	0.142	0.000
water				
water	0.000	0.000	0.000	1.000

in selected binary solvent–IL mixtures leads to qualitative predictions of the phase behavior of the molecule in any mixture. We then present results of data-fitting against γ^∞ values for 35 organic solvents in 22 different ionic liquids. We also analyze the resulting NRTL-SAC molecular descriptors for these ILs and compare the molecular parameters against the chemical structure of the ILs. Last, we show that the NRTL-SAC molecular descriptors can be used to provide robust qualitative predictions for the phase behavior of the ILs with various organic solvents.

The 35 organic solvents investigated in this study were chosen because their NRTL-SAC molecular descriptors have been identified previously and are readily available.⁸ Table 1 shows the list of these 35 organic solvents and their corresponding NRTL-SAC parameters for hydrophobicity (X), solvation strength (Y−), polarity (Y+), and hydrophilicity (Z). These 35 solvents are mainly alkanes, aromatics, ketones, alcohols, ethers, esters, and chlorohydrocarbons. They are representatives of organic solvents used in the pharmaceutical industry for either process development purposes such as polymorph determination or manufacturing of active pharmaceutical ingredients. It should be noted that the application of the NRTL-SAC method is in no way limited to those organic solvents listed in Table 1. Rather, the methodology is applicable to any solvents or molecules with molecular descriptors that can be reliably

identified from experimental phase equilibrium or infinite-dilution activity coefficient data.

Table 2 shows the list of the 22 ionic liquids investigated in this study and the literature data sources for γ^∞ of the various organic solvents in the ILs. Among the 22 ionic liquids, there are actually only 19 unique ones. Three ionic liquids have data reported by different research groups. In this study, we choose to treat them as “different” ionic liquids to examine the sensitivity of the NRTL-SAC model to the potential variations in the quality of the experimental measurements.

Many organic electrolytes, behaving similarly to ionic liquids, may form molecular ion pairs when dissolved in solution. Although the aim of this study is to investigate the applicability of NRTL-SAC to ionic liquids, the knowledge gained from this study will help validate the applicability of the NRTL-SAC methodology to organic electrolytes in general. This new knowledge is particularly interesting and significant in view of the general lack of experimental data for organic electrolytes. Future work will involve applying the electrolyte version of the NRTL-SAC model to IL containing systems.

NRTL Segment Activity Coefficient Model. The NRTL-SAC model computes activity coefficients from a combinatorial term and a residual term.

$$\ln \gamma_I = \ln \gamma_I^C + \ln \gamma_I^R \quad (1)$$

The combinatorial term γ_I^C is calculated from the Flory–Huggins equation for the combinatorial entropy of mixing. The residual term γ_I^R is calculated from the local composition (lc) contribution γ_I^{lc} of the polymer NRTL model.¹² Incorporating the segment interaction concept, the equation computes the activity coefficient for component *I* in solution by summing up contributions to the activity coefficient from all segments that make up component *I*.

$$\ln \gamma_I^R = \ln \gamma_I^{lc} = \sum_i r_{i,I} [\ln \Gamma_i^{lc} - \ln \Gamma_{i,I}^{lc}] \quad (2)$$

$$\ln \Gamma_i^{lc} = \frac{\sum_j x_j G_{ji} \tau_{ji}}{\sum_k x_k G_{ki}} + \sum_l \frac{x_l G_{il}}{\sum_k x_k G_{kl}} \left(\tau_{il} - \frac{\sum_j x_j G_{jl} \tau_{jl}}{\sum_k x_k G_{kl}} \right) \quad (3)$$

$$\ln \Gamma_{i,I}^{lc} = \frac{\sum_j x_{j,I} G_{ji} \tau_{ji}}{\sum_k x_{k,I} G_{ki}} + \sum_l \frac{x_{l,I} G_{il}}{\sum_k x_{k,I} G_{kl}} \left(\tau_{il} - \frac{\sum_j x_{j,I} G_{jl} \tau_{jl}}{\sum_k x_{k,I} G_{kl}} \right) \quad (4)$$

where *I* is the component index, *i*, *j*, *k*, and *l* are the segment species indices, $r_{i,I}$ is the number of segment species *i* contained only in component *I*, Γ_i^{lc} is the activity coefficient of segment species *i*, $\Gamma_{i,I}^{lc}$ is the activity coefficient of segment species *i* contained only in component *I*, x_j is the segment-based mole fraction of segment species *j*, and $x_{j,I}$ is the segment-based mole fraction of segment species *j* contained only in component *I*. *G* and τ in eq 3 and eq 4 are binary quantities related to each other by α , i.e., $G = \exp(-\alpha\tau)$. α and τ are the nonrandomness factor parameter and the segment–segment binary interaction energy parameter, respectively. The exact expressions for x_j and $x_{j,I}$ are given in the Chen and Song article.⁶

Chen and Song⁶ also introduced four unique “conceptual” segments that broadly characterize various surface interaction characteristics of molecules. These four conceptual segments, together with their corresponding nonrandomness factor and segment–segment binary interaction energy parameters (i.e., α and τ), are capable of qualitatively describing the various

Table 2. List of Ionic Liquids Studied and Literature Data Sources for Infinite-Dilution Activity Coefficients

IL No.	IL Full Name	Structure	IL Short Name	References	Note
1	1-ethyl-3-methyl-imidazolium bis(trifluoromethylsulfonyl)imide		[emim][Tf ₂ N]	[13]	
2	1-butyl-3-methyl-imidazolium bis(trifluoromethylsulfonyl)imide		[bmim][Tf ₂ N]	[13]	
3	1,3-dimethyl-imidazolium dimethylphosphate		[mmim][(CH ₃) ₂ PO ₄]	[13]	
4	1-hexyl-3-methyl-imidazolium bis(trifluoromethylsulfonyl)imide		[hmim][Tf ₂ N]	[14]	
5	1-methyl-3-octyl-imidazolium bis(trifluoromethylsulfonyl)imide		[omim][Tf ₂ N]	[14]	
6	1-butyl-1-methyl-pyrrolidinium bis(trifluoromethylsulfonyl)imide		[bmpyr][Tf ₂ N]	[14]	
7	1-butyl-4-methyl-pyridinium tetrafluoroborate		[bmpy][BF ₄]	[23, 24]	
8	1-ethyl-3-methyl-imidazolium bis-(trifluoromethylsulfonyl) imide		[emim][Tf ₂ N]	[25]	same as IL #1
9	1,2-dimethyl-3-ethyl-imidazolium bis(trifluoromethylsulfonyl) imide		[emmim][Tf ₂ N]	[25]	
10	1-butyl-3-methyl-imidazolium bis(trifluoromethylsulfonyl) imide		[bmim][Tf ₂ N]	[26]	same as IL #2
11	1-methyl-3-octyl-imidazolium tetrafluoroborate		[omim][BF ₄]	[27]	

Table 2. Continued

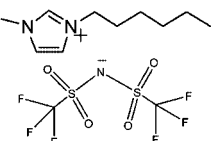
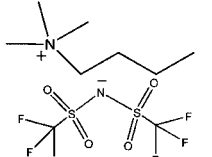
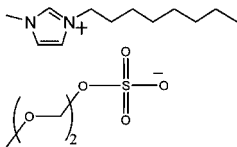
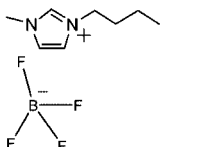
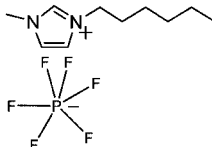
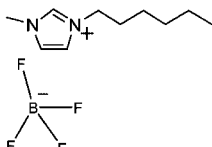
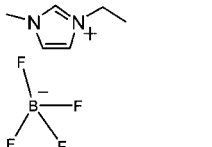
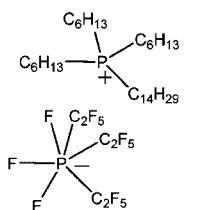
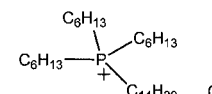
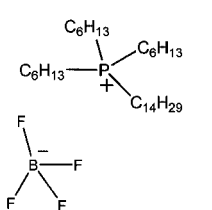
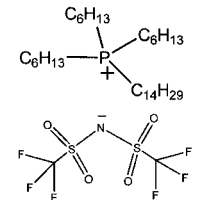
12	1-hexyl-3-methyl-imidazolium bis(trifluoromethylsulfonyl) imide		[hmim][Tf ₂ N]	[28, 29]
13	trimethyl-butylammonium bis(trifluoromethylsulfonyl) imide		[Me ₃ BuN][Tf ₂ N]	[30]
14	1-methyl-3-octyl-imidazolium diethyleneglycolmonomethylethersulfate		[omim][DEGSO ₄]	[31]
15	1-butyl-3-methyl-imidazolium tetrafluoroborate		[bmim][BF ₄]	[32, 33]
16	1-hexyl-3-methyl-imidazolium hexafluorophosphate		[hmim][PF ₆]	[34]
17	1-hexyl-3-methyl-imidazolium tetrafluoroborate		[hmim][BF ₄]	[35]
18	1-ethyl-3-methyl-imidazolium tetrafluoroborate		[emim][BF ₄]	[36]
19	Trihexyl-tridecyl-phosphonium tris(pentafluoroethyl) trifluorophosphate		[thtd-Ph] [(C ₂ F ₅) ₃ PF ₃]	[1]
20	Trihexyl-tridecylphosphonium chloride		[thtd-Ph][Cl]	[4]
21	Trihexyl-tridecylphosphonium tetrafluoroborate		[thtd-Ph][BF ₄]	[4]
22	Trihexyl-tridecylphosphonium bis(trifluoromethylsulfonyl) imide		[thtd-Ph][Tf ₂ N]	[4]

Table 3. NRTL-SAC Molecular Descriptors Identified for Ionic Liquids

IL no.	IL	X	Y−	Y+	Z	temperature (K)	R ²	no. of data points
1	[emim][Tf ₂ N]	0.000	0.000	2.240	0.941	353.15	0.954	4
2	[bmim][Tf ₂ N]	0.000	0.235	3.576	0.782	353.15	1.000	3
3	[mmim][(CH ₃) ₂ PO ₄]	0.000	0.015	0.000	0.153	353.15	0.826	5
4	[hmim][Tf ₂ N]	0.320	0.000	3.908	0.405	303.15	0.933	26
5	[omim][Tf ₂ N]	0.326	0.447	4.740	0.000	303.15	0.889	12
6	[bmpyr][Tf ₂ N]	0.000	0.000	4.444	0.197	303.15	0.964	9
7	[bmpy][BF ₄]	0.000	0.062	1.224	0.158	298.15	0.790	27
8	[emim][Tf ₂ N]	0.000	0.000	2.861	0.271	298.15	0.887	27
9	[emmim][Tf ₂ N]	0.000	0.000	2.634	0.063	298.15	0.865	28
10	[bmim][Tf ₂ N]	0.000	0.000	3.725	0.205	298.15	0.943	19
11	[omim][BF ₄]	0.252	0.000	1.135	0.387	298.15	0.926	23
12	[hmim][Tf ₂ N]	0.196	0.000	4.296	0.000	298.15	0.928	22
13	[Me ₃ BuN][Tf ₂ N]	0.000	0.000	2.541	0.177	298.15	0.917	24
14	[omim][DEGSO ₄]	0.163	0.468	5.074	2.490	298.15	0.972	7
15	[bmim][BF ₄]	0.000	0.000	1.024	0.339	298.15	0.824	29
16	[hmim][PF ₆]	0.000	0.000	2.888	0.351	298.15	0.919	7
17	[hmim][BF ₄]	0.000	0.000	3.937	1.241	298.15	0.940	7
18	[emim][BF ₄]	0.000	0.000	0.454	5.211	363.65	0.983	4
19	[thtd-Ph][(C ₂ F ₅) ₃ PF ₃]	3.733	0.000	4.691	0.448	308.15	0.852	9
		3.848	0.000	4.811	0.550	318.15	0.857	9
		3.959	0.000	4.632	0.719	328.15	0.855	9
20	[thtd-Ph][Cl]	3.897	0.024	1.170	1.247	308.15	0.973	8
		3.955	0.002	1.173	1.269	318.15	0.973	8
		3.992	0.000	1.175	1.278	328.15	0.972	8
21	[thtd-Ph][BF ₄]	2.466	0.000	1.819	0.000	308.15	0.985	8
		2.553	0.000	1.903	0.000	318.15	0.986	8
		2.618	0.000	1.989	0.000	328.15	0.987	8
22	[thtd-Ph][Tf ₂ N]	3.666	0.000	1.184	1.108	308.15	0.963	8
		3.712	0.000	1.170	1.098	318.15	0.964	8
		3.729	0.000	1.157	1.079	328.15	0.965	8

molecular interactions and the corresponding phase behaviors. Specifically, it was proposed to describe the molecular surface interactions of all solvents and solutes in solution by using hydrophobic, solvation, polar, and hydrophobic segments. The conceptual segment numbers for each molecule are measures of the effective molecular surface areas that exhibit surface interaction characteristics of hydrophobicity (X), solvation strength (Y−), polarity (Y+), and hydrophilicity (Z). These molecule-specific conceptual segment numbers, or molecular descriptors, correspond to $r_{i,l}$ in eq 2.

Chen and Song⁶ further proposed “reference compounds” for the conceptual segments. The reference compounds are used to identify the segment–segment nonrandomness factor and binary interaction energy parameters for the conceptual segments from regression of available experimental vapor–liquid and liquid–liquid equilibrium data associated with these reference compounds.

To determine the molecular descriptors for a molecule, phase equilibrium data for at least four binary systems containing the molecule and solvents or solutes of varied surface interaction characteristics are needed. The parametrization is improved if the binary systems contain a range of hydrophilic solvents, polar solvents, solvation solvents, and hydrophobic solvents. Once the molecular descriptors are determined, the NRTL-SAC model can provide robust qualitative predictions for phase behaviors of mixtures containing the molecule as long as the molecular descriptors for other species in the mixture are also known.

Correlation of Infinite-Dilution Activity Coefficient Data. The data on infinite-dilution activity coefficients of the organic solvents in the ILs were taken from the papers summarized in Table 2, and they were regressed to identify the molecular descriptors for the ILs. Some papers reported γ^∞ values for solvents at multiple temperatures. To limit the scope of this study, wherever available, we chose to focus on γ^∞ values at 298.15 K only because it is not the purpose of this study to determine the partial molar excess enthalpy at infinite dilution for the solvent, $\bar{H}^{e,\infty}$. We did, however, determine the molecular

descriptors from γ^∞ values at multiple temperatures for the four phosphonium-based ILs in Table 2 (i.e., ILs 19–22) to examine the temperature dependency of the molecular descriptors for the ILs.

Table 3 summarizes the correlation results for γ^∞ data of the solvents in the 22 ionic liquids (19 unique ILs). During the regression, in order to treat the γ^∞ data from various sources in a consistent manner, all γ^∞ data were assumed to have a relative standard deviation of 10%, a reasonable estimate of standard deviation for γ^∞ data. For each ionic liquid system, Table 3 shows the identified NRTL-SAC molecular descriptors for the IL, the number of experimental data points, the corresponding temperature for the γ^∞ data, and the squared correlation coefficient, R^2 . It should be emphasized that the NRTL-SAC molecular descriptors can be well identified from a very small set of data points (three to four) as long as these data points offer a variety of solvent characteristics in terms of hydrophobicity, polarity, hydrophilicity, etc.

Table 3 shows that the γ^∞ data for the solvents in the ILs are all satisfactorily correlated with NRTL-SAC. With the exception of IL 3 ([mmim][(CH₃)₂PO₄]), IL 7 ([bmpy][BF₄]), and IL 15 ([bmim][BF₄]), the correlation coefficients of R^2 are better than 0.85. It is significant that for many of the ILs these γ^∞ data can be correlated satisfactorily with only two or three molecular descriptors.

Table 3 further shows that, in the context of NRTL-SAC, these ionic liquids show “hybrid” molecular surface characteristics with various degrees of hydrophobicity, polarity, and hydrophilicity. The four phosphonium-based ILs (IL 19–22) are highly hydrophobic, reflecting the long alkyl chains (three hexyl and one tetradecyl) present in the phosphonium-based cation. In contrast, the imidazolium-based ILs show little or no hydrophobicity with the exception of some ILs, i.e., IL 4 ([hmim][Tf₂N]), IL 5 ([omim][Tf₂N]), IL 11 ([omim][BF₄]), IL 12 ([hmim][Tf₂N]), and IL 14 ([omim][DEGSO₄]) that show

small degrees of hydrophobicity due to their larger alkyl chains attached to the imidazolium moiety.

Among the 22 ILs, IL 3, [mmim][(CH₃)₂PO₄], seems to be an interesting exception. The γ^∞ data for IL 3 are relatively poorly represented, as reflected by one of the worst correlation coefficients. It has molecular descriptors of zero hydrophobicity, zero polarity and rather small degrees of solvation strength and hydrophilicity. Such poor representation of the γ^∞ data and relatively meaningless molecular descriptors may be indicative of failure of NRTL-SAC for this IL or breakdown of the assumption that the IL would form molecular ion pairs and exhibit phase behavior of that of molecular species. In other words, [mmim][(CH₃)₂PO₄] may behave more like an electrolyte and form individual ions in lieu of molecular ion pairs in the solvents.

As mentioned before, there are two [emim][Tf₂N] systems (IL 1 and IL 8), two [bmim][Tf₂N] systems (IL 2 and IL 10), and two [hmim][Tf₂N] systems (IL 4 and IL 12) in Table 3. They represent infinite-dilution activity coefficient data for these three ILs from different sources and at different temperatures. Table 3 shows that the NRTL-SAC molecular descriptors for these duplicate ILs do share similar values (with high polarity, low hydrophobicity, and low hydrophilicity) even though they were identified from different data sources with potentially different quality experimental measurements and at different temperatures. For example, in the specific case of IL 1 and IL 8, Table 3 reports *Z* to be 0.941 for IL 1 and 0.271 for IL 8. What is significant from the NRTL-SAC model perspective is that the *Z*'s are small (low hydrophilicity) in comparison to *Y*+ (high polarity). The difference of 0.67 reflects the variation in experimental measurements by different groups and the uncertainties in the parameters with relatively small absolute values.

Table 3 also shows the identified molecular descriptors from solvent γ^∞ values at multiple temperatures for the four phosphonium-based ILs (ILs 19–22). The results clearly show that the solvent γ^∞ data are well represented at all temperatures, and as a first approximation, it may be assumed that the molecular descriptors for the ILs are relatively independent of temperature. This is perhaps not surprising since the solvent γ^∞ data are also relatively invariant for each solvent over the temperature range measured.^{1,4}

Figures 1–6 show correlated versus experimental values of $\ln \gamma^\infty$ for solvents in the two [emim][Tf₂N] IL systems, the two [bmim][Tf₂N] IL systems, and the two [hmim][Tf₂N] IL systems. It is worth noting that, among various solvent types, the NRTL-SAC predictions of $\ln \gamma^\infty$ for alkylbenzenes are consistently on the high side in comparison to the experimental data. It suggests either the NRTL-SAC parameters in Table 1 should be further optimized for alkylbenzenes or the molecular species representation for ionic liquids is less satisfactory for ILs in alkylbenzenes.

Note that, in treating the infinite-dilution activity coefficient data, for IL 12, [hmim][Tf₂N], the data point for 1,4-dioxane is found to be a significant outlier and it is excluded from the regression. Likewise, for IL 13, [Me₃BuN][Tf₂N], the data point for *N*-methylpyrrolidone is found to be a significant outlier and it is not used in the regression. Figure 6 shows the correlation results for IL 12, [hmim][Tf₂N]. The excluded data point for 1,4-dioxane is such an outlier that it actually lies outside the figure.

Prediction of Phase Behavior. With the NRTL-SAC molecular descriptors identified for the ILs, the model is now used to predict the phase behavior of various mixtures involving the ILs. Table 4 summarizes available VLE and LLE data and the

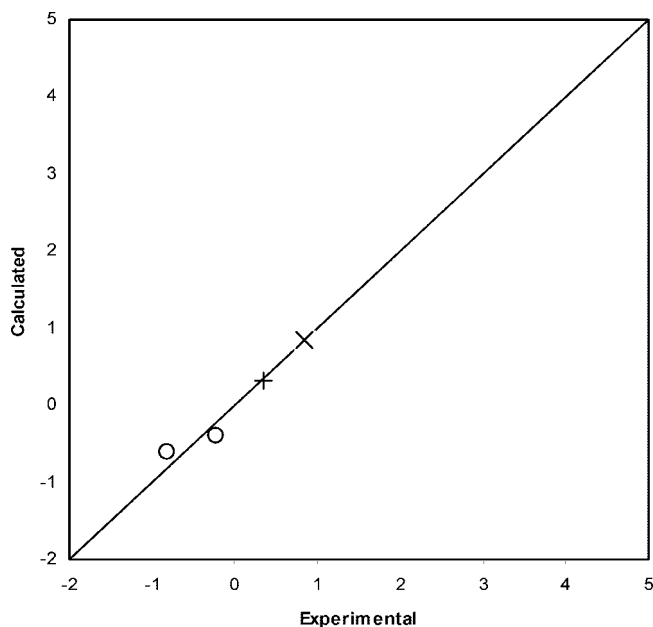


Figure 1. Calculated versus experimental $\ln \gamma^\infty$ data of Kato and Gmehling¹³ for solvents in the ionic liquid 1 ([emim][Tf₂N]) at 353.15 K with $R^2 = 0.954$: +, alcohols; O, polar organics; and x, water.

corresponding literature sources for the ILs considered in this investigation. A significant amount of VLE data is available for the imidazolium-based ILs with the [Tf₂N] anion. Of particular interest are the extensive VLE data sets associated with IL 1 ([emim][Tf₂N]) and IL 2 ([bmim][Tf₂N]), not only in pure solvents but also in acetone/2-propanol and 2-propanol/water binary mixtures. Given that, with the exception of IL 3 ([mmim][(CH₃)₂PO₄]), all imidazolium-based ILs listed in Table 3 exhibit largely similar surface interaction characteristics, i.e., with high polarity and mixed degrees of hydrophilicity, we choose to focus on VLE predictions with IL 1 ([emim][Tf₂N]) and IL 2 ([bmim][Tf₂N]). Their VLE phase behavior should provide good examples for the imidazolium-based ILs that can be satisfactorily described with the polarity and hydrophilicity parameters. In the discussion to follow, first binary and ternary

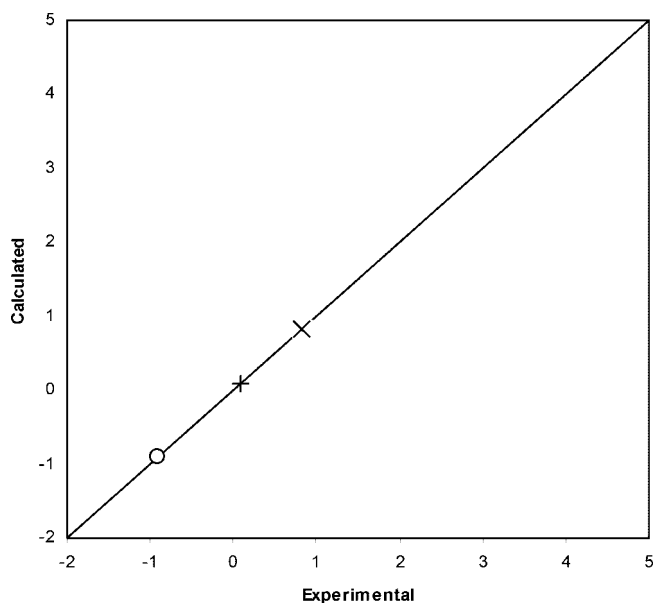


Figure 2. Calculated versus experimental $\ln \gamma^\infty$ data of Kato and Gmehling¹³ for solvents in the ionic liquid 2 ([bmim][Tf₂N]) at 353.15 K with $R^2 = 1.000$: +, alcohols; O, polar organics; and x, water.

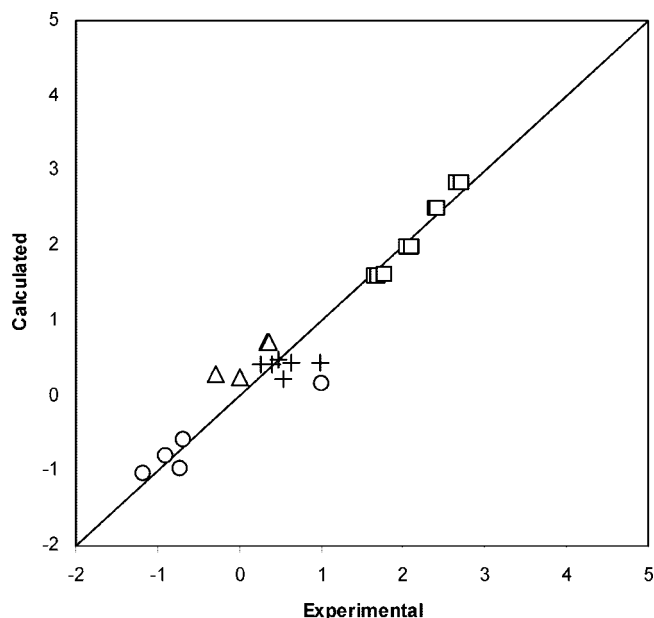


Figure 3. Calculated versus experimental $\ln \gamma^\infty$ data of Kato and Gmehling¹⁴ for solvents in the ionic liquid 4 ([hmim][Tf₂N]) at 303.15 K with $R^2 = 0.933$: □, alkanes; Δ, alkylbenzenes; +, alcohols; and ○, polar organics.

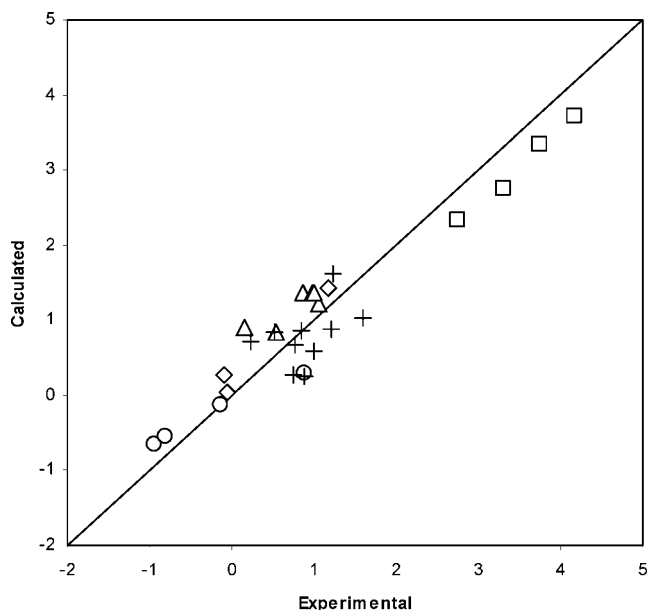


Figure 4. Calculated versus experimental $\ln \gamma^\infty$ data of Heintz et al.²⁵ for solvents in the ionic liquid 8 ([emim][Tf₂N]) at 298.15 K with $R^2 = 0.887$: □, alkanes; Δ, alkylbenzenes; +, alcohols; ○, polar organics; and ◇, chloromethanes.

VLE predictions followed by ternary LLE predictions with the NRTL-SAC model are examined.

Figure 7 shows the predicted vapor–liquid equilibrium for acetone, 2-propanol, tetrahydrofuran, and water with [emim][Tf₂N] at 353.15 K. NRTL-SAC predictions match well with the experimental data of Kato and Gmehling¹³ for the acetone/[emim][Tf₂N] binary, the 2-propanol/[emim][Tf₂N] binary, and the water/[emim][Tf₂N] binary. The model is able to predict the existence of the miscibility gap for the water–[emim][Tf₂N] binary, consistent with the experimental observation, which is indicated by the vapor pressure curve becoming flat at ~0.7 mol fraction of water. However, the model underpredicts the vapor pressure for the tetrahydrofuran/[emim][Tf₂N] binary.

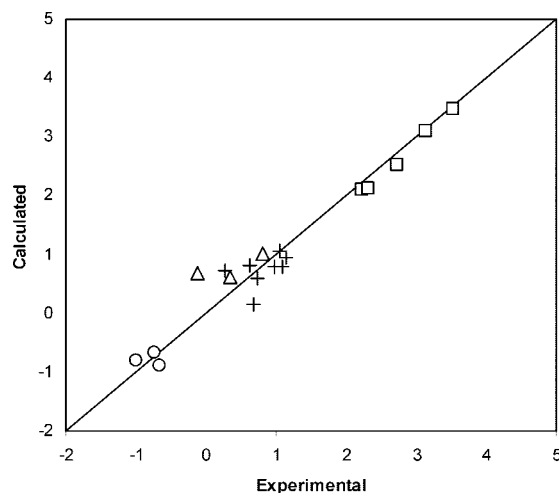


Figure 5. Calculated versus experimental $\ln \gamma^\infty$ data of Heintz et al.²⁶ for solvents in the ionic liquid 10 ([bmim][Tf₂N]) at 298.15 K with $R^2 = 0.943$: □, alkanes; Δ, alkylbenzenes; +, alcohols; and ○, polar organics.

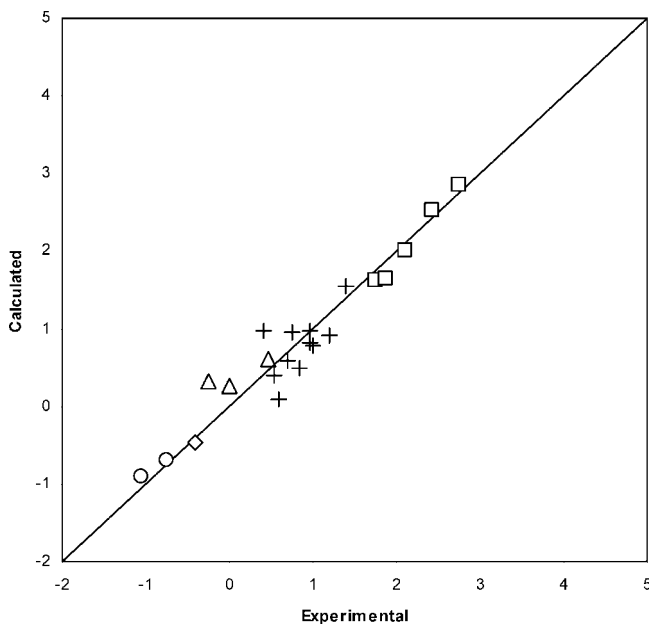


Figure 6. Calculated versus experimental $\ln \gamma^\infty$ data of Heintz and Verevkin²⁸ for solvents in the ionic liquid 12 ([hmim][Tf₂N]) at 298.15 K with $R^2 = 0.928$: □, alkanes; Δ, alkylbenzenes; +, alcohols; ○, polar organics; and ◇, chloromethanes.

Figure 8 shows the predicted vapor–liquid equilibrium for methanol and ethanol with [emim][Tf₂N] at 353.15 K. NRTL-SAC predictions match well with the experimental data of Kato and Gmehling¹⁴ for both binaries. Figure 9 further shows the predicted vapor–liquid equilibrium for hexane, cyclohexane, and benzene with [emim][Tf₂N] at 353.15 K. The model correctly predicts the existence of miscibility gaps for these three binaries with [emim][Tf₂N], as reported by Kato et al.,¹⁵ although the model predicts much larger miscibility gap than the data indicate for the benzene–[emim][Tf₂N] system, consistent with the earlier observation that the NRTL-SAC predictions of $\ln \gamma^\infty$ for alkylbenzenes are on the high side in comparison to the experimental data.

Figures 10 and 11 show the predicted VLE at 353.15 K for the acetone/2-propanol/[emim][Tf₂N] ternary system and the 2-propanol/water/[emim][Tf₂N] ternary system, respectively. The model predictions capture the trends very well as shown

Table 4. Summary of Literature VLE and LLE Data

IL no.	IL	IL systems with VLE and LLE data	temperature/pressure	refs
1	[emim][Tf ₂ N]	acetone-IL, 2-propanol-IL, water-IL binary systems, and acetone-2-propanol-IL and 2-propanol-water-IL ternary systems (VLE)	353.15 K	16
		acetone-IL, 2-propanol-IL, tetrahydrofuran-IL, water-IL binary systems (VLE)	353.15 K	13
		hexane-IL, cyclohexane-IL, benzene-IL binary systems (VLE)	353.15 K	15
		methanol-IL, ethanol-IL binary systems (VLE)	~353.15 K	14
		benzene-hexane-IL ternary system (LLE)	298.15 and 313.15 K	17
2	[bmim][Tf ₂ N]	acetone-IL, 2-propanol-IL, water-IL binary systems, and acetone-2-propanol-IL and 2-propanol-water-IL ternary systems (VLE)	353.15 K	16
		acetone-IL, 2-propanol-IL, water-IL binary systems (VLE)	353.15 K	13
		cyclohexane-IL, benzene-IL binary systems (VLE)	353.15 K	15
		methanol-IL, ethanol-IL, 1-propanol-IL, benzene-IL binary systems (VLE)	298.15–313.15 K	37
3	[mmim][(CH ₃) ₂ PO ₄]	1-butanol-water-IL ternary system (cloud point)	288 K	19
		methanol-IL, ethanol-IL, acetone-IL, tetrahydrofuran-IL, and water-IL binary systems (VLE)	353.15 K	13
		ethanol–water-IL ternary system (VLE)	101.32 kPa	38
		methanol-ethanol-IL and ethanol-water-IL ternary systems (VLE)	300–330 K	39
4	[hmim][Tf ₂ N]	cyclohexane-IL, methanol-IL, ethanol-IL binary systems (VLE)	~353.15 K	14
		1-butanol-water-IL and ethanol–water-IL ternary systems (LLE)	298.15 K	20
5	[omim][Tf ₂ N]			
6	[bmpyr][Tf ₂ N]			
7	[bmpy][BF ₄]			
8	[emim][Tf ₂ N]	(same as IL 1)		
9	[emmim][Tf ₂ N]			
10	[bmim][Tf ₂ N]	(same as IL 2)		
11	[omim][BF ₄]	methanol-IL, ethanol-IL, 1-propanol-IL, benzene-IL binary systems (VLE)	298.15–313.15 K	40
12	[hmim][Tf ₂ N]	(same as IL 4)		
13	[Me ₃ BuN][Tf ₂ N]	methanol-IL, ethanol-IL, 1-propanol-IL binary systems (VLE)	298.15–313.15 K	30
14	[omim][DEGSO ₄]			
15	[bmim][BF ₄]			
16	[hmim][PF ₆]			
17	[hmim][BF ₄]			
18	[emim][BF ₄]	water-tetrahydrofuran-IL ternary system (LLE)	337.15 K	21
19	[thtd-Ph][(C ₂ F ₅) ₃ PF ₃]			
20	[thtd-Ph][Cl]			
21	[thtd-Ph][BF ₄]			
22	[thtd-Ph][Tf ₂ N]			

in the experimental data of Doker and Gmehling.¹⁶ In fact, the NRTL-SAC predictions for the two ternaries are better than those predicted with the Wilson, NRTL and UNIQUAC equations by Doker and Gmehling.¹⁶ It should be emphasized

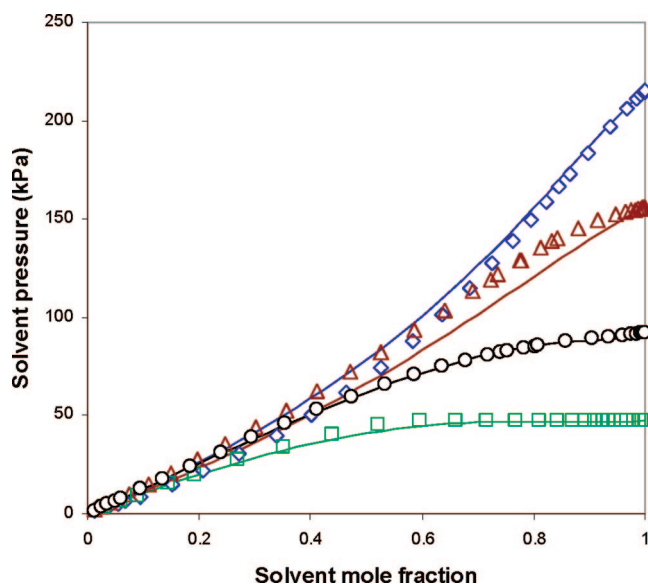


Figure 7. Predicted versus experimental vapor–liquid equilibrium data of Kato and Gmehling¹³ for the binary solvent/[emim][Tf₂N] systems at 353.15 K: (◇) acetone experimental data, (○) 2-propanol experimental data, (□) water experimental data, (Δ) tetrahydrofuran experimental data, and (—) NRTL-SAC.

that the Wilson, NRTL, and UNIQUAC predictions by Doker and Gmehling¹⁶ are based on binary interaction parameters identified from the available experimental VLE data for the binary systems. In the case of NRTL-SAC, the predictions are based on pure component IL molecular descriptors identified

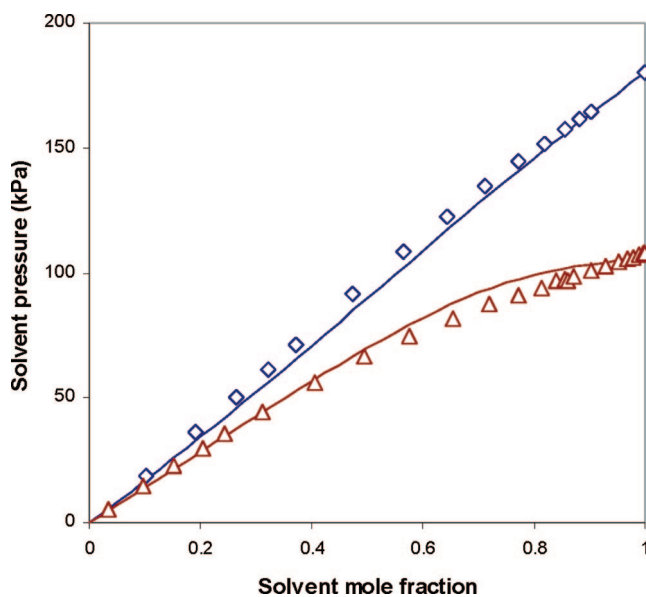


Figure 8. Predicted versus experimental vapor–liquid equilibrium data of Kato and Gmehling¹⁴ for the binary solvent/[emim][Tf₂N] systems at 353.15 K: (◇) methanol experimental data, (Δ) ethanol experimental data, and (—) NRTL-SAC.

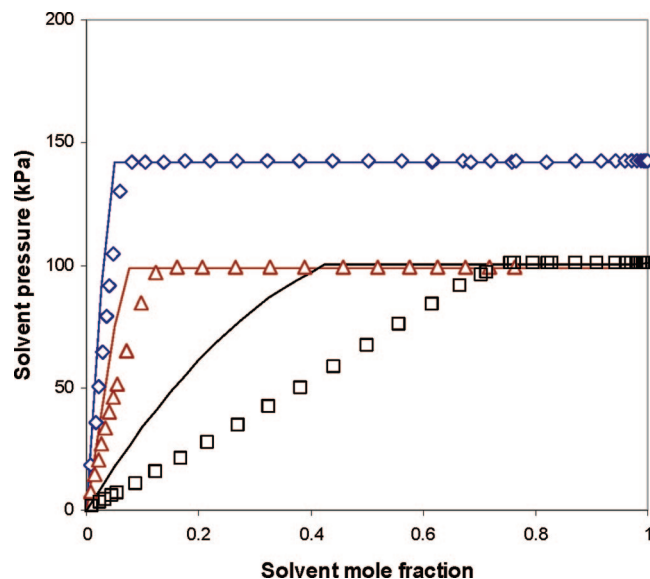


Figure 9. Predicted versus experimental vapor-liquid equilibrium data of Kato et al.¹⁵ for the binary solvent/[emim][Tf₂N] systems at 353.15 K: (◇) hexane experimental data, (Δ) cyclohexane experimental data, (□) benzene experimental data, and (—) NRTL-SAC.

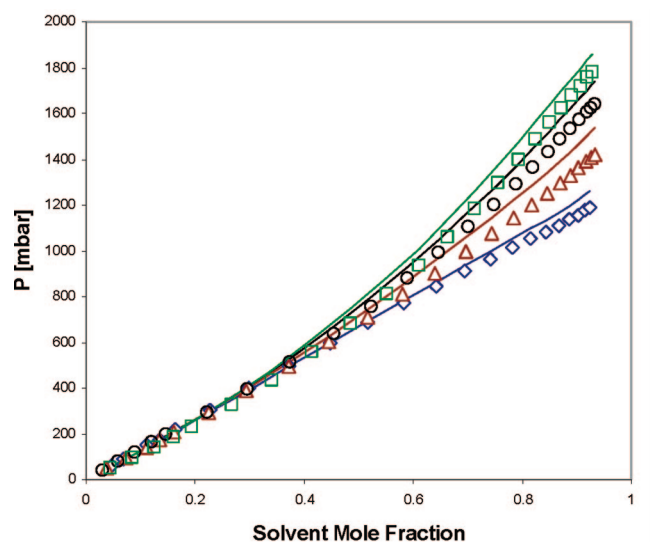


Figure 10. Predicted versus experimental vapor-liquid equilibrium data of Doker and Gmehling¹⁶ for the ternary system acetone/2-propanol/[emim][Tf₂N] at 353.15 K: (◇) 20.59 mol % acetone experimental data, (Δ) 39.95 mol % acetone experimental data, (○) 60.65 mol % acetone experimental data, (□) 78.78 mol % acetone experimental data, and (—) NRTL-SAC. The solvent mole fraction scale represents the combined mole fractions of acetone and 2-propanol.

only from the infinite-dilution activity coefficients of organic solvents in the ILs, as shown in Table 3. Doker and Gmehling¹⁶ reported relative root-mean-square deviations (rmsd) of 9.79 and 5.78% with the Wilson model, 8.50 and 8.61% with the NRTL model, and 10.27 and 5.28% with the UNIQUAC model, for the acetone/2-propanol/[emim][Tf₂N] ternary system and the 2-propanol/water/[emim][Tf₂N] ternary system, respectively. The relative root-mean-square deviations are 6.07 and 4.66% with the NRTL-SAC model for the same two ternaries. Note that the relative root-mean-square deviation is calculated by using the following equation:

$$\text{rmsd (\%)} = 100 \sqrt{\frac{1}{n} \sum_n \left(\frac{P_{\text{exp}} - P_{\text{calc}}}{P_{\text{exp}}} \right)^2} \quad (5)$$

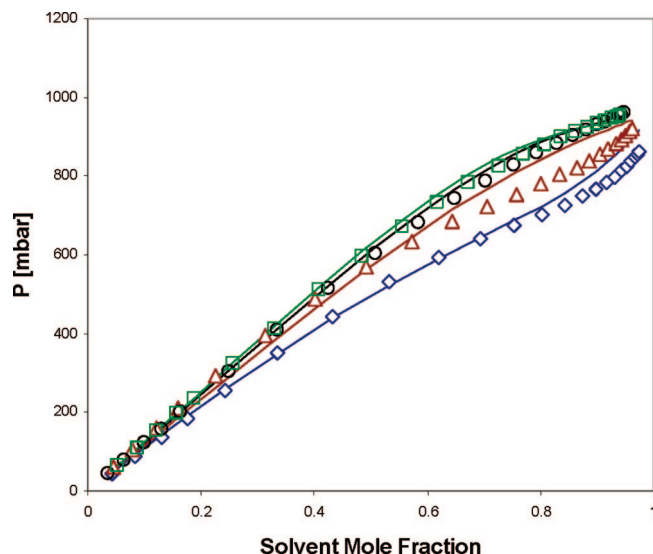


Figure 11. Predicted versus experimental vapor-liquid equilibrium data of Doker and Gmehling¹⁶ for the ternary system 2-propanol/water/[emim][Tf₂N] at 353.15 K: (◇) 19.92 mol % 2-propanol experimental data, (Δ) 41.20 mol % 2-propanol experimental data, (○) 59.75 mol % 2-propanol experimental data, (□) 80.04 mol % 2-propanol experimental data, and (—) NRTL-SAC. The solvent mole fraction scale represents the combined mole fractions of 2-propanol and water.

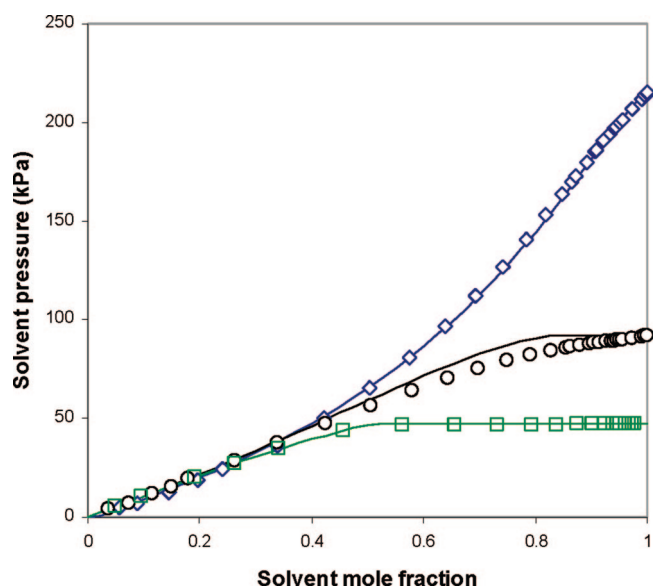


Figure 12. Predicted versus experimental vapor-liquid equilibrium data of Kato and Gmehling¹³ for the binary solvent/[bmim][Tf₂N] systems at 353.15 K: (◇) acetone experimental data, (○) 2-propanol experimental data, (□) water experimental data, and (—) NRTL-SAC.

Here P_{exp} and P_{calc} are the experimental and calculated pressure values, respectively, and the sum is over all data points.

Figure 12 shows the predicted vapor-liquid equilibrium for acetone, 2-propanol, and water with [bmim][Tf₂N] at 353.15 K. In comparison to the experimental data of Kato and Gmehling,¹³ the NRTL-SAC predictions match the experimental data reasonably well. A miscibility gap is predicted for the water/[bmim][Tf₂N] binary, consistent with the experimental observation. NRTL-SAC also predicts a miscibility gap for the 2-propanol-[bmim][Tf₂N] binary, while the data show no such immiscibility. This suggests that NRTL-SAC overpredicts activity coefficients for 2-propanol in the 2-propanol-[bmim][Tf₂N] binary.

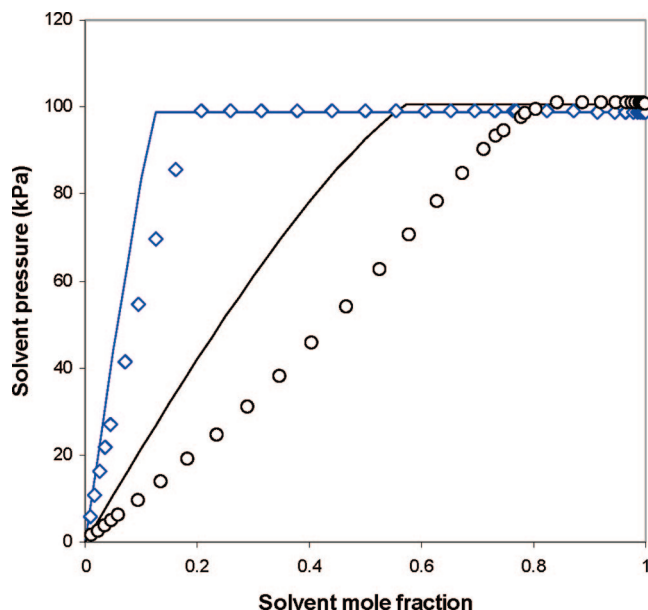


Figure 13. Predicted versus experimental vapor-liquid equilibrium data of Kato et al.¹⁵ for the binary solvent/[bmim][Tf₂N] systems at 353.15 K: (◇) cyclohexane experimental data, (○) benzene experimental data, and (—) NRTL-SAC.

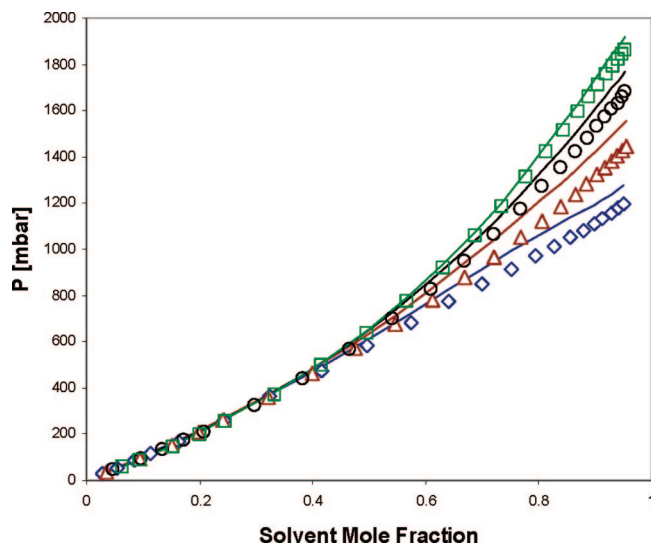


Figure 14. Predicted versus experimental vapor-liquid equilibrium data of Docker and Gmehling¹⁶ for the ternary system acetone/2-propanol/[bmim][Tf₂N] at 353.15 K: (◇) 19.10 mol % acetone experimental data, (Δ) 38.69 mol % acetone experimental data, (○) 59.85 mol % acetone experimental data, (□) 80.25 mol % acetone experimental data, and (—) NRTL-SAC. The solvent mole fraction scale represents the combined mole fractions of acetone and 2-propanol.

Figure 13 shows the predicted vapor-liquid equilibrium for cyclohexane and benzene with [bmim][Tf₂N] at 353.15 K. The model predicts the existence of miscibility gaps for both the cyclohexane/[bmim][Tf₂N] binary and benzene/[bmim][Tf₂N] binary, consistent with the data of Kato et al.,¹⁵ although quantitative agreement is lacking for the benzene/[bmim][Tf₂N] binary. Again, this is consistent with the earlier observation that the NRTL-SAC predictions of $\ln \gamma^\infty$ for alkylbenzenes are on the high side in comparison to the experimental data.

Figures 14 and 15 show the predicted VLE at 353.15 K for the acetone/2-propanol/[bmim][Tf₂N] ternary system and the 2-propanol/water/[bmim][Tf₂N] ternary system, respectively. Similar to the results for the [emim][Tf₂N] ternaries, the model predictions capture well the vapor pressure trends as shown in

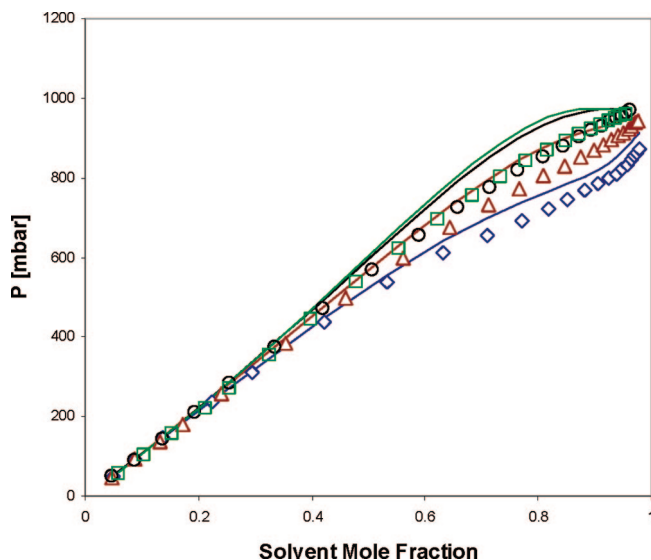


Figure 15. Predicted versus experimental vapor-liquid equilibrium data of Docker and Gmehling¹⁶ for the ternary system 2-propanol/water/[bmim][Tf₂N] at 353.15 K: (◇) 21.28 mol % 2-propanol experimental data, (Δ) 40.47 mol % 2-propanol experimental data, (○) 59.25 mol % 2-propanol experimental data, (□) 80.54 mol % 2-propanol experimental data, and (—) NRTL-SAC. The solvent mole fraction scale represents the combined mole fractions of 2-propanol and water.

the experimental data of Docker and Gmehling.¹⁶ The NRTL-SAC predictions for the two ternaries are in line or slightly worse than with those predicted with the Wilson, NRTL, and UNIQUAC equations. Docker and Gmehling¹⁶ reported rmsd of 2.61% and 4.26% with the Wilson model, 2.42% and 9.35% with the NRTL model, and 2.77% and 1.77% with the UNIQUAC model, for the acetone/2-propanol/[bmim][Tf₂N] ternary system and the 2-propanol/water/[bmim][Tf₂N] ternary system, respectively. The relative root-mean-square deviations are 5.33% and 5.80% with the NRTL-SAC model for the same two ternaries.

For the four ternary systems studied by Docker and Gmehling,¹⁶ the average rmsd errors are 5.61% with Wilson, 7.22% with NRTL, and 5.02% with UNIQUAC. The average rmsd error is 5.46% with NRTL-SAC. Clearly, for these ternary systems, the NRTL-SAC VLE prediction results are on a par with those predicted with the Wilson, NRTL, and UNIQUAC equations, each of which involves model parameters that were fit to binary VLE data.

Experimental LLE data are available for the ternary system benzene/hexane/[emim][Tf₂N] at 298.15 K,¹⁷ a type 2 system indicating a single-phase envelope spanning the entire diagram between two binary miscibility gaps.¹⁸ Figure 16 shows the NRTL-SAC predictions versus the experimental data. With the IL 1 parameters and the IL 8 parameters of Table 3, NRTL-SAC gives very good type 2 predictions. As shown in Table 3, IL 1 and 8 parameters were estimated using γ^∞ data at 353 and 298 K, respectively. It is obvious upon viewing Figure 16 that the prediction using IL 8 is more accurate. In this case, both solvent/[emim][Tf₂N] binary miscibility gaps are more accurately predicted, and the IL molecular descriptors were identified with γ^∞ data at the same temperature as that of the experimental LLE data. In both predictions, the predicted binodal curves are very close to the experimental data although the slopes of the tie lines are off significantly. Furthermore, neither prediction anticipates a solutrope (the point where tie line slope changes direction), which is apparent in the experimental data.

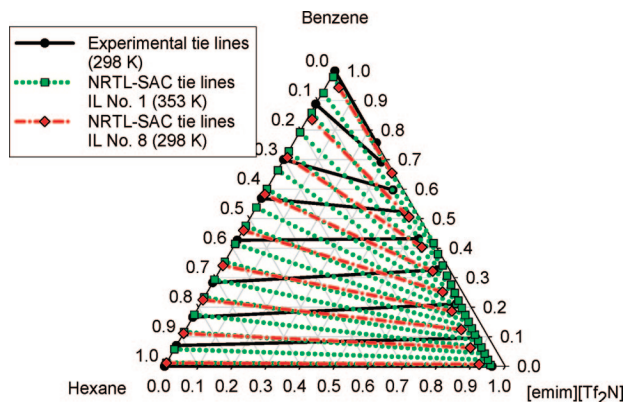


Figure 16. Predicted versus experimental liquid–liquid equilibrium data of Arce et al.¹⁷ for the ternary system benzene/hexane/[emim][Tf₂N] at 298.15 K.

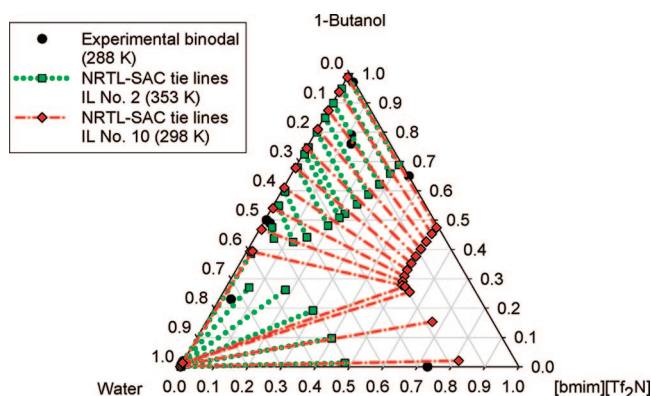


Figure 17. Predicted versus experimental liquid–liquid equilibrium data of Najdanovic-Visak et al.¹⁹ for the ternary system 1-butanol/water/[bmim][Tf₂N].

Figure 17 shows the NRTL-SAC predictions versus the experimental LLE data of Najdanovic-Visak et al.¹⁹ for the ternary system 1-butanol/water/[bmim][Tf₂N]. The experimental data suggest the system is type 3b at 288 K, which denotes three distinct phase envelopes emanating from three binary miscibility gaps.¹⁸ NRTL-SAC predictions are made with IL 2 and IL 10 parameters for [bmim][Tf₂N], which were determined from γ^∞ data at 353 and 298 K, respectively. Depending on the IL parameters used, the NRTL-SAC model predicts differing qualitative behavior. With IL 2 parameters, the LLE ternary prediction is type 3a, where there is a single-phase envelope connecting the water/1-butanol and water/IL binary miscibility gaps and a single distinct phase envelope corresponding to the 1-butanol/IL binary.¹⁸ This type 3a prediction is encouraging, as predicting complete miscibility at intermediate compositions is challenging for these types of systems. Using IL 10 parameters from Table 3 results in a type 3 system, which is characterized by a three-phase region. Furthermore, we observe that the predictions yield increasingly miscible behavior as the temperature at which the IL molecular descriptors were estimated increases. This behavior is in line with IL/*n*-alcohol/water systems commonly exhibiting upper critical solution temperature behavior.

Figures 18 and 19 show the NRTL-SAC predictions versus the experimental LLE data of Chapeaux et al.²⁰ for the ternary system ethanol/water/[hmim][Tf₂N] and the ternary system 1-butanol/water/[hmim][Tf₂N]. Both experimental data sets were measured at 295 K. The experimental data suggest type 1 for the ternary system ethanol/water/[hmim][Tf₂N] and type 2 for

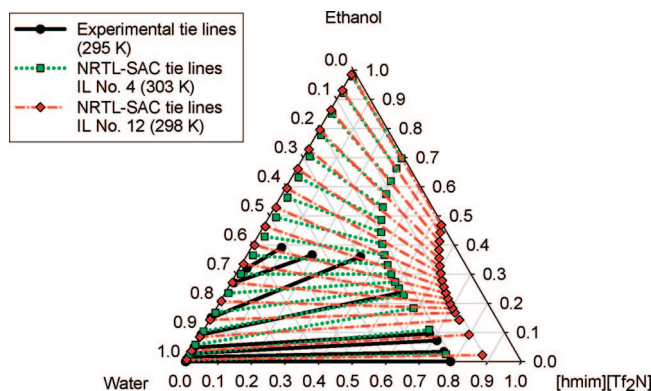


Figure 18. Predicted versus experimental liquid–liquid equilibrium data of Chapeaux et al.²⁰ for the ternary system ethanol/water/[hmim][Tf₂N].

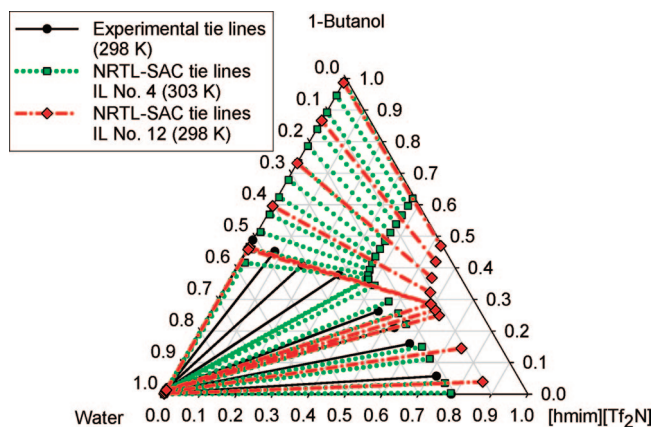


Figure 19. Predicted versus experimental liquid–liquid equilibrium data of Chapeaux et al.²⁰ for the ternary system 1-butanol/water/[hmim][Tf₂N].

the ternary system 1-butanol/water/[hmim][Tf₂N]. For both systems, NRTL-SAC predictions were performed using parameters for both IL 4 and IL 12, determined from γ^∞ data at 303 and 298 K, respectively. For both sets of molecular descriptors, NRTL-SAC incorrectly predicts type 2 for the ternary system ethanol/water/[hmim][Tf₂N] and type 3 for the ternary system 1-butanol/water/[hmim][Tf₂N]. The source of the incorrect predictions is the predicted miscibility gap for the alcohol/[hmim][Tf₂N] binaries. Again, it should be noted that, in both cases, the predicted miscibility increases (phase envelopes become smaller) as the temperature at which the IL molecular descriptors were obtained increases. Finally, the quantitative accuracy of the water/[hmim][Tf₂N] and 1-butanol/water binary miscibility gaps is encouraging.

Figure 20 shows the NRTL-SAC predictions versus the experimental LLE data of Jork et al.²¹ measured at 337 K for the ternary system tetrahydrofuran/water/[emim][BF₄]. The experimental data suggest type 1 for the ternary system, and NRTL-SAC also correctly predicts type 1 (a single, distinct phase envelope with a plait point)¹⁸ using the molecular descriptors for IL 18, which were estimated from only four γ^∞ data points at 363 K. Although the predicted phase envelope is considerably smaller than the observed phase envelope, the tie line slopes are quite accurate. This is an important aspect of the prediction as it correctly indicates [emim][BF₄]'s ability to extract water from a tetrahydrofuran-rich phase.

Based on the studies shown above, it is clear that NRTL-SAC is a promising tool in predicting both binary VLE and the existence of binary LLE miscibility gaps. The qualitative and, in some cases, near-quantitative ternary LLE predictions are

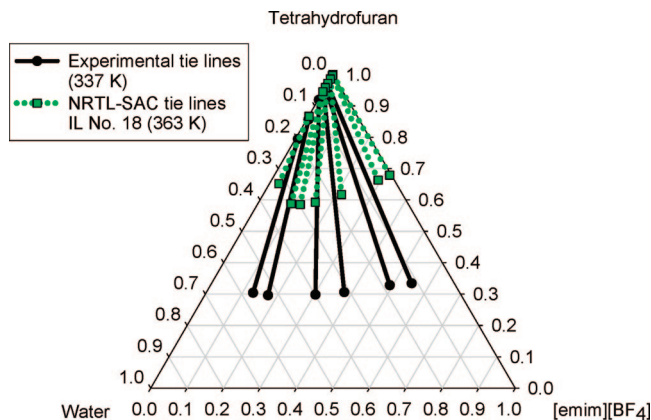


Figure 20. Predicted versus experimental liquid–liquid equilibrium data of Jork et al.²¹ for the ternary system tetrahydrofuran/water/[emim][BF₄].

notable since NRTL-SAC is a purely predictive model that requires only pure component molecular descriptors. Although the NRTL-SAC ternary LLE predictions (based on IL parameters determined only from γ^∞ data) are of lesser quality than those made by some other conventional g^E models that are fit directly to finite composition VLE and LLE binary data,²² significant insight can be taken from these NRTL-SAC predictions for liquid separations.

Conclusions

The NRTL-SAC model is successfully used to describe qualitatively the phase behavior of ionic liquids. With the exception of one ionic liquid, [mmim][(CH₃)₂PO₄], which appears to not be described well as a molecular ion pair, the model satisfactorily correlates values of infinite-dilution activity coefficients of 35 different solvents in 22 ionic liquids at various temperatures. The resulting NRTL-SAC molecular descriptors for the ionic liquids suggest these IL species are mainly polar molecules with various degrees of hydrophobicity and hydrophilicity. We further show that NRTL-SAC predicts qualitatively the phase behavior of binary and ternary solvent–ionic liquid systems including vapor–liquid equilibrium, binary liquid–liquid miscibility gaps, and ternary liquid–liquid equilibrium. In fact, the VLE model predictions for the ternary systems with the molecule-specific NRTL-SAC parameters are on par with the results obtained with the Wilson, NRTL, and UNIQUAC models, which use binary-specific parameters. Furthermore, NRTL-SAC is a promising predictive tool in determining the existence of binary LLE miscibility gaps, which have been predicted via both VLE calculations and LLE calculations. NRTL-SAC should be very useful as a correlation and prediction tool in the development of novel ionic liquids with different degrees of hydrophobicity, polarity, solvation strength, and hydrophilicity.

Acknowledgment

This work was supported in part by the Department of Energy under Grant DE-FG02-05CH11294. Additional support was provided by a University of Notre Dame Arthur J. Schmitt Presidential Fellowship (L.D.S.).

Literature Cited

(1) Letcher, T. M.; Reddy, P. Determination of Activity Coefficients at Infinite Dilution of Organic Solutes in the Ionic Liquid, trihexyl(tetradecyl)-

phosphonium tris(pentafluoroethyl) trifluorophosphate, by Gas-Liquid Chromatography. *Fluid Phase Equilib.* **2005**, *235*, 11–17.

(2) Diedenhofen, M.; Eckert, F.; Klamt, A. Prediction of Infinite Dilution Activity Coefficients of Organic Compounds in Ionic Liquids Using COSMO-RS. *J. Chem. Eng. Data* **2003**, *48*, 475–479.

(3) Eike, D. M.; Brennecke, J. F.; Maginn, E. J. Predicting Infinite-Dilution Activity Coefficients of Organic Solutes in Ionic Liquids. *Ind. Eng. Chem. Res.* **2004**, *43*, 1039–1048.

(4) Banerjee, T.; Khanna, A. Infinite Dilution Activity Coefficients for Trihexyltetradecyl Phosphonium Ionic Liquids: Measurements and COSMO-RS Predictions. *J. Chem. Eng. Data* **2006**, *51*, 2170–2177.

(5) Freire, M. G.; Santos, L. M. N. B. F.; Marrucho, I. M.; Coutinho, J. A. P. Evaluation of COSMO-RS for the Prediction of LLE and VLE of Alcohols + Ionic Liquids. *Fluid Phase Equilib.* **2007**, *255*, 167–178.

(6) Chen, C.-C.; Song, Y. Solubility Modeling with a Nonrandom Two-Liquid Segment Activity Coefficient Model. *Ind. Eng. Chem. Res.* **2004**, *43*, 8354–8362.

(7) Chen, C.-C.; Song, Y. Extension of NonRandom Two-Liquid Segment Activity Coefficient Model for Electrolytes. *Ind. Eng. Chem. Res.* **2005**, *44*, 8909–8921.

(8) Chen, C.-C.; Crafts, P. A. Correlation and Prediction of Drug Molecule Solubility in Mixed Solvent Systems with the NonRandom Two-Liquid Segment Activity Coefficient (NRTL-SAC) Model. *Ind. Eng. Chem. Res.* **2006**, *45*, 4816–4824.

(9) Tung, H.-H.; Tabora, J.; Variankaval, N.; Bakken, D.; Chen, C.-C. Prediction of Pharmaceutical Solubility via NRTL-SAC and COSMO-SAC. *J. Pharm. Sci.* **2008**, *97*, 1813–1820.

(10) Mullins, E.; Liu, Y.-A.; Ghaderi, A.; Fast, S. D. Sigma Profile Database for Predicting Solid Solubility in Pure and Mixed Solvent Mixtures for Organic Pharmacological Compounds with COSMO-Based Thermodynamic Models. *Ind. Eng. Chem. Res.* **2008**, *47*, 1707–1725.

(11) Kokitkar, P. B.; Plocharczyk, E.; Chen, C.-C. Modeling Drug Molecule Solubility to Identify Optimal Solvent Systems for Crystallization. *Org. Process Res. Dev.* **2008**, *12*, 249–256.

(12) Chen, C.-C. A Segment-Based Local Composition Model for the Gibbs Energy of Polymer Solutions. *Fluid Phase Equilib.* **1993**, *83*, 301–312.

(13) Kato, R.; Gmehling, J. Measurement and Correlation of Vapor-Liquid Equilibria of Binary Systems Containing the Ionic Liquids [EMIM][(CF₃SO₂)₂N], [BMIM][(CF₃SO₂)₂N], [MMIM][(CH₃)₂PO₄] and Oxygenated Organic Compounds Respectively. *Fluid Phase Equilib.* **2005**, *231*, 38–43.

(14) Kato, R.; Gmehling, J. Systems with Ionic Liquids: Measurement of VLE and γ^∞ Data and Prediction of Their Thermodynamic Behavior Using Original UNIFAC, Mod. UNIFAC(Do) and COSMO-RS(O1). *J. Chem. Thermodyn.* **2005**, *37*, 603–619.

(15) Kato, R.; Krummen, M.; Gmehling, J. Measurement and Correlation of Vapor-Liquid Equilibria and Excess Enthalpies of Binary Systems Containing Ionic Liquids and Hydrocarbons. *Fluid Phase Equilib.* **2004**, *224*, 47–54.

(16) Doker, M.; Gmehling, J. Measurement and Prediction of Vapor-Liquid Equilibria of Ternary Systems Containing Ionic Liquids. *Fluid Phase Equilib.* **2005**, *227*, 255–266.

(17) Arce, A.; Earle, M. J.; Rodriguez, H.; Seddon, K. R. Separation of Aromatic Hydrocarbons from Alkanes Using the Ionic Liquid 1-Ethyl-3-methylimidazolium bis(trifluoromethyl) sulfonyl]amide. *Green Chem.* **2007**, *9*, 70–74.

(18) Sørensen, J. M.; Arlt, W., *Liquid-Liquid Equilibrium Data Collection*; DECHEMA: Frankfurt/Main, Germany, 1979.

(19) Najdanovic-Visak, V.; Rebelo, L. P. N.; da Ponte, M. N. Liquid-Liquid Behavior of Ionic Liquid-1-Butanol-Water and High Pressure CO₂-Induced Phase Changes. *Green Chem.* **2005**, *7*, 443–450.

(20) Chapeaux, A.; Simoni, L. D.; Ronan, T. S.; Stadtherr, M. A.; Brennecke, J. F. Extraction of Alcohols from Water with 1-n-Hexyl-3-methylimidazolium bis(trifluoromethylsulfonyl) imide. Submitted to *Green Chem.*

(21) Jork, C.; Seiler, M.; Beste, Y.-A.; Arlt, W. Influence of Ionic Liquids on the Phase Behavior of Aqueous Azeotropic Systems. *J. Chem. Eng. Data* **2004**, *49*, 852–857.

(22) Simoni, L. D.; Lin, Y.; Brennecke, J. F.; Stadtherr, M. A. Modeling Liquid-Liquid Equilibrium of Ionic Liquid Systems with NRTL, Electrolyte NRTL, and UNIQUAC. *Ind. Eng. Chem. Eng.* **2008**, *47*, 256–272.

(23) Heintz, A.; Kulikov, D. V.; Verevkin, S. P. Thermodynamic Properties of Mixtures Containing Ionic Liquids. 1. Activity Coefficients at Infinite Dilution of Alkanes, Alkenes, and Alkylbenzenes in 4-Methyl-n-Butylpyridinium Tetrafluoroborate Using Gas-Liquid Chromatography. *J. Chem. Eng. Data* **2001**, *46*, 1526–1529.

(24) Heintz, A.; Kulikov, D. V.; Verevkin, S. P. Thermodynamic Properties of Mixtures Containing Ionic Liquids. Activity Coefficients at

Infinite Dilution of Polar Solutes in 4-Methyl-n-Butylpyridinium Tetrafluoroborate Using Gas-Liquid Chromatography. *J. Chem. Thermodyn.* **2002**, *34*, 1341–1347.

(25) Heintz, A.; Kulikov, D. V.; Verevkin, S. P. Thermodynamic Properties of Mixtures Containing Ionic Liquids. 2. Activity Coefficients at Infinite Dilution of Hydrocarbons and Polar Solutes in 1-Methyl-3-ethyl-imidazolium Bis(trifluoromethyl-sulfonyl) Amide and in 1,2-Dimethyl-3-ethyl-imidazolium Bis(trifluoromethyl-sulfonyl) Amide Using Gas-Liquid Chromatography. *J. Chem. Eng. Data* **2002**, *47*, 894–899.

(26) Heintz, A.; Casas, L. M.; Nesterov, I. A.; Emel'yanenko, V. N.; Verevkin, S. P. Thermodynamic Properties of Mixtures Containing Ionic Liquids. 5. Activity Coefficients at Infinite Dilution of Hydrocarbons, Alcohols, Esters, and Aldehydes in 1-Methyl-3-butyl-imidazolium Bis(trifluoromethyl-sulfonyl) Imide Using Gas-Liquid Chromatography. *J. Chem. Eng. Data* **2005**, *50*, 1510–1514.

(27) Heintz, A.; Verevkin, S. P. Thermodynamic Properties of Mixtures Containing Ionic Liquids. 6. Activity Coefficients at Infinite Dilution of Hydrocarbons, Alcohols, Esters, and Aldehydes in 1-Methyl-3-octyl-imidazolium Tetrafluoroborate Using Gas-Liquid Chromatography. *J. Chem. Eng. Data* **2005**, *50*, 1515–1519.

(28) Heintz, A.; Verevkin, S. P. Thermodynamic Properties of Mixtures Containing Ionic Liquids. 8. Activity Coefficients at Infinite Dilution of Hydrocarbons, Alcohols, Esters, and Aldehydes in 1-Hexyl-3-methyl-imidazolium Bis(trifluoromethyl-sulfonyl) Imide Using Gas-Liquid Chromatography. *J. Chem. Eng. Data* **2006**, *51*, 434–437.

(29) Heintz, A.; Verevkin, S. P.; Lehmann, J. K.; Vasil'tsova, T. V.; Ondo, D. Activity Coefficients at Infinite Dilution and Enthalpies of Solution of Methanol, 1-Butanol, and 1-Hexanol in 1-Hexyl-3-methyl-imidazolium Bis(trifluoromethyl-sulfonyl) Imide. *J. Chem. Thermodyn.* **2007**, *39*, 268–274.

(30) Heintz, A.; Vasil'tsova, T. V.; Safarov, J.; Bich, E.; Verevkin, S. P. Thermodynamic Properties of Mixtures Containing Ionic Liquids. 9. Activity Coefficients at Infinite Dilution of Hydrocarbons, Alcohols, Esters, and Aldehydes in Trimethyl-butylammonium Bis(trifluoromethyl-sulfonyl) Imide Using Gas-Liquid Chromatography and Static Method. *J. Chem. Eng. Data* **2006**, *51*, 648–655.

(31) Deenadayalu, N.; Thango, S. H.; Letcher, T. M.; Ramjugernath, D. Measurement of Activity Coefficients at Infinite Dilution Using Polar and Non-polar Solutes in the Ionic Liquid 1-Methyl-3-octyl-imidazolium Diethyleneglycol-monomethylethersulfate at T=(288.15, 298.15 and 313.15) K. *J. Chem. Thermodyn.* **2006**, *38*, 542–546.

(32) Zhou, Q.; Wang, L.-S. Activity Coefficients at Infinite Dilution of Alkanes, Alkenes, and Alkyl Benzenes in 1-Butyl-3-methyl-imidazolium Tetrafluoroborate Using Gas-Liquid Chromatography. *J. Chem. Eng. Data* **2006**, *51*, 1698–1701.

(33) Zhou, Q.; Wang, L.-S.; Wu, J.-S.; Li, M.-Y. Activity Coefficients at Infinite Dilution of Polar Solutes in 1-Butyl-3-methyl-imidazolium Tetrafluoroborate Using Gas-Liquid Chromatography. *J. Chem. Eng. Data* **2007**, *52*, 131–134.

(34) Letcher, T. M.; Soko, B.; Ramjugernath, D.; Deenadayalu, N.; Nevines, A.; Naicker, P. K. Activity Coefficients at Infinite Dilution of Organic Solutes in 1-Hexyl-3-methyl-imidazolium Hexafluorophosphate from Gas-Liquid Chromatography. *J. Chem. Eng. Data* **2003**, *48*, 708–711.

(35) Letcher, T. M.; Soko, B.; Reddy, P.; Deenadayalu, N. Determination of Activity Coefficients at Infinite Dilution of Solutes in the Ionic Liquid 1-Hexyl-3-methyl-imidazolium Tetrafluoroborate Using Gas-Liquid Chromatography at the Temperatures 298.15 K and 323.15 K. *J. Chem. Eng. Data* **2003**, *48*, 1587–1590.

(36) Jork, C.; Kristen, C.; Pieraccini, D.; Stark, A.; Chiappe, C.; Beste, Y. A.; Arlt, W. Tailor-Made Ionic Liquids. *J. Chem. Thermodyn.* **2005**, *37*, 537–558.

(37) Verevkin, S. P.; Safarov, J.; Bich, E.; Hassel, E.; Heintz, A. Thermodynamic Properties of Mixtures Containing Ionic Liquids. Vapor Pressures and Activity Coefficients of n-Alcohols and Benzene in Binary Mixtures with 1-Methyl-3-Butyl-Imidazolium Bis(trifluoromethyl-sulfonyl) Imide. *Fluid Phase Equilib.* **2005**, *236*, 222–228.

(38) Zhao, J.; Dong, C.-C.; Li, C.-X.; Meng, H.; Wang, Z.-H. Isobaric Vapor-Liquid Equilibria for Ethanol-Water System Containing Different Ionic Liquids at Atmospheric Pressure. *Fluid Phase Equilib.* **2006**, *242*, 147–153.

(39) Zhao, J.; Li, C.-X.; Wang, Z.-H. Vapor Pressure Measurement and Prediction for Ethanol-Methanol and Ethanol-Water Systems Containing Ionic Liquids. *J. Chem. Eng. Data* **2006**, *51*, 1755–1760.

(40) Safarov, J.; Verevkin, S. P.; Bich, E.; Heintz, A. Vapor Pressures and Activity Coefficients of n-Alcohols and Benzene in Binary Mixtures with 1-Methyl-3-butyl-imidazolium Octyl Sulfate and 1-Methyl-3-octyl-imidazolium Tetrafluoroborate. *J. Chem. Eng. Data* **2006**, *51*, 518–525.

Received for review January 15, 2008

Revised manuscript received May 5, 2008

Accepted June 24, 2008

IE800048D